

## An Autonomous Wheelchair with Indoor Positioning System and Smart 3D Headphone for the Visually Impaired

João S. Pereira<sup>1,2,3</sup>, Gurukiran Manjunath<sup>1</sup>, Nuno Almeida<sup>1</sup>, Sílvia P. Mendes<sup>1,3</sup>

(1) Polytechnic Institute of Leiria, School of Technology and Management,

(2) Instituto de Telecomunicações, Portugal,

(3) Center for research in Informatics and Communications,  
Leiria, Portugal.

Corresponding Author: João S. Pereira

**Abstract:** Much research on electric-powered wheelchairs (EPWs) has been carried out in recent years to mitigate the problems of disabled people. We have come a long way since the basic manually-operated wheelchairs, and the progress made has considerably improved freedom of mobility of the disabled. This study proposes an autonomous EPW (electric powered wheelchair) having smart driving features for the visually impaired. Our initial prototype, the Instituto Politécnico de Leiria/Instituto de Telecomunicações (IPL/IT) wheelchair had voice, eye-movement, and GPS (Global Positioning System) control. Our latest version which we propose in this paper includes an Indoor locating system (IPS) using 3D printed directional Wi Fi antennas that allow a precise positioning of the wheelchair in an indoor scenario and a novel smart 3D headphone that can generate acoustic signals in proportion to a 3D object, which will allow the visually impaired to identify the size and shape of obstacles, and thus, avoid them. The IPL/IT EPW system has been designed with low-cost IoT (Internet of Things) technology in mind.

**Keywords:** indoor positioning system, autonomous wheelchair, Internet of Things (IoT), telemedicine, tele-assistance, visually-impaired, seeing with 3D sounds.

Date of Submission: 21-01-2019

Date of acceptance: 05-02-2019

### I. INTRODUCTION

One of the most frequently used assistive vehicle for improving the personal movement of people with disabilities is the wheelchair. The availability of wheelchairs that are suitable, well-made, and equipped not only improves mobility, but also opens the way to education, employment, and better prospects for disabled people [1]. Wheelchairs are thus an important part of daily lives as they can positively influence the quality of life for people with diminished mobility [2]. In most cases, manual or electric powered wheelchairs (EPW) are adequate. However, in instances where there is a lack of independent mobility, for example, in people with impaired vision, tremors, visual field reduction, spasticity, or intellectual impairment, wheelchair usage requires some assistance. Other research works [3, 4] focus on smart wheelchairs that can plot a route to a desired destination without the intervention of the user. A smart or autonomous wheelchair can be defined as “a uniquely modified powered wheelchair which is equipped with a control system and variant sensors” [4]. It can otherwise be called a robot base with an affixed seat that can move [5].

The objective of smart wheelchairs is to assist users who have some form of impairment that prevents them from navigating the wheelchair on their own, or who require the wheelchair to navigate autonomously to a chosen location, such as individuals with serious mobility impairments or who are visually impaired. The main purpose is to reduce or eliminate the user’s task in navigating the wheelchair. Moreover, an EPW design needs to be customized to the user’s condition and impairment.

Two variants of smart wheelchairs are acknowledged: a regular power wheelchair with an added on-board computer and a collection of sensors, and a moveable robot base with an affixed seat [5].

Presently, most commercially available smart wheelchairs are power wheelchairs which have been considerably modified, such as MAid (Mobility Aid for Elderly and Disabled people), NavChair, OMNI (Office wheelchair with high Manoeuvrability and Navigational Intelligence), and SENARIO [6–9]. Other smart wheelchairs such as Hephaestus, TinMan, Siamo, Smart Wheelchair Component System (SWCS), and Smart Power Assistance Module (SPAM) are designed as auxiliary units that can be joined to and removed from the base wheelchair infrastructure [10–14]. Generally, attention is required in two important areas for the design of an autonomous wheelchair. These are customisability and taking safety requirements into account [15].

Customizability means that the design of a smart wheelchair considers the needs of potential users in general, and also incorporates the flexibility to be modified to suit the needs of a specific individual, in particular.

In general, an autonomous wheelchair's primary functions and suitable operational units are: user interface, navigation, and obstacle recognition and evasion [15]. Methods used for user interface in autonomous wheelchairs include various types of joysticks (e.g., standard, force-feedback, etc.), chin or head control, sip-and-puff devices, user facial expressions, and voice recognition [7, 8, 16–20]. Sensors are used to identify and evade obstacles. Multiple sensors may be used in a single wheelchair such as cameras for image processing, various kinds of range finders such as ultrasonic (sonar), infra-red (IR), and laser (LRF), bump sensors, and optical fiber gyroscopes [21–23]. Smart wheelchairs can vary in the manner of navigation assistance they offer, e.g. from the ability to follow targets to being limited to simple collision avoidance [8, 24]. Also, they may use an internal map to independently navigate to a specified destination. Tracks may also be used to facilitate autonomous navigation [25].

Many kinds of locating systems have been developed to estimate an autonomous mobile robot's absolute position in an indoor set-up [26]. In one study [27], a laser range finder was used to estimate a mobile robot position which identified artificial landmarks positioned in the environment. In another study [28], data gathered from the ultrasonic sensors of the robot was matched with an environmental global map for calculating its position. Additionally, studies have been conducted using radio frequency (RF) operated systems for determining the location of mobile robots [29, 30]. In [29], movable objects estimate their location by employing the Time-of-Arrival technique (TOA). The Q-Track [30] system uses moving objects that send signals to fixed receivers. This information is sent to a central unit which calculates the object location. The effectiveness of RF Indoor Positioning Systems is limited due to multiple reflections of the sent signal.

A novel headphone that simulates reflected sound waves from obstacles into 3D acoustic signals has also been developed.

Some manufacturers have software that turns a headset into visual aids for the blind by changing images snapped by a camera into sounds that the user's brain can reconstruct into pictures [31][32]. The vOICE system [32] translates images into sounds in real-time. Once per second, the computer scans a 64x64 pixel frame. Each pixel in a column produces a wave whose frequency indicates its position; the highest frequencies are at the top. The sound waves are produced based on the 16-tone grey scale amplitudes of each pixel. Once all data has been extracted, the referred system grabs and digitizes a new video frame that orients the listener. To further boost the spatial orientation of the listener, stereo headphones are used to shift the volume balance from left-to-right in step with the movement of the pixel scanner. This gives the person a sense of the location of the objects. A low-resolution camera was chosen for capturing the images because the human ear has a lower capacity than the eye for handling data [32].

The next section presents a design and an implementation of our new autonomous wheelchair. The section III is related to the triangulation process used to locate the wheelchair. The section IV shows a new method based on sound conversion of 3D objects for the IPL/IT EPW that may help the visually impaired. Finally, the section V presents some conclusions.

## **II. DESIGN AND IMPLEMENTATION OF THE NEW AUTONOMOUS WHEELCHAIR**

The hardware components of the proposed IPL/IT autonomous EPW is shown in Fig. 1 and Fig. 2. The primary system control is achieved by a Raspberry Pi minicomputer. The movement of the EPW is carried out by two DC motors with speed controllers. A simple joystick module steers the EPW. Speed, voice and eye motion is used as a complement or replacement of the joystick. The custom software, manages all the peripheral sensing devices. The images, which are collected by a webcam, also assess user intent by reading eye motion. Two instruction sets were created for eye-movements: direction and halting of all movements. In addition to tracking ocular movements, validating voice commands, and an autopilot were included in the system. Figure 3 presents our graphical user interface. A personalized voice recognition application for voice controlling was integrated with the motors and is managed by the mini-computer. Instructions for directional motion and halting are managed by a voice command algorithm. As the wheelchair prototype uses a Raspberry Pi minicomputer, the DC motors can be controlled using such a voice recognition module to move in accordance to the voice commands. The voice command algorithm "Correlation of Spectrograms", applied to our IPL/IT wheelchair, was developed [34] by João S. Pereira, in 2001.



**Figure 1:** Block diagram of proposed system



**Figure 2:** The low cost autonomous IPL/IT wheelchair system, with voice command, eye movement detection, GPS, colored line follower, and sound produced by scanned objects

The IPL/IT wheelchair system contains manual controls for Front, Left, Right, and Reverse movements. Additionally, the wheelchair has smart commands, such as reading eye movements, with a webcam fixed on a helmet; validation by voice commands using a microphone; autopilot using a Global Positioning System (GPS) or a colored line; and autopilot via Internet (Web). Moreover, the IPL/IT wheelchair system is low priced (lower than 400€) and is a modular system that can be modified to suit with any wheelchair. Furthermore, its controls are configurable to any user.



Figure 3: Graphic interface of the eye-controlled system

The hardware design for the novel 3D surround headset system is illustrated in Fig. 4. The system, added to the IPL/IT wheelchair, comprises of (1) three pairs of speakers, (2) an image-based 3D scanner, and (3) an ultrasonic 3D scanner. A ©Microsoft Kinect 3D scanner is used when the object is visible to the user; else the ultrasonic 3D scanner is used. This ©Microsoft Kinect 3D scanner has been incorporated in our IPL/IT autonomous wheelchair. The sound system will explained in section IV.



Figure 4: 3D surround headphones schematics

The Raspberry Pi minicomputer serves as the heart of the system and offers an interface between the GPS module and the collision avoidance sensors. The wheelchair system receives latitude and longitude information through a GPS module. We display this information on Google Maps by using Google application programming interfaces (API). Figure 5 illustrates our graphic user interface. A mobile app offers both an enriched experience to the user and handy information regarding the location of the wheelchair. The app communicates on a real-time basis with the server. We refresh the data (latitude and longitude) at intervals of 1 second. The positioning system also has the capability to regulate the movements of the wheelchair and its direction/orientation. The data is registered and documented in a defined format.



Figure 5: Locating Wheelchair on Google Map

Therefore, our IPS wheelchair system includes:

1. A web server running on Raspberry Pi,
2. A mobile phone which uses a browser to view images from the webcam of the wheelchair, and
3. A server-provided web page which
  - i. permits dynamic commands for real-time control of the two motors of the wheelchair,
  - ii. offers supplementary information regarding the different sensors utilized to avert issues, such as collisions (ultrasonic sensors and a Kinect scanner), and
  - iii. Gives the IPS location of the wheelchair.

The GPS works well in an outdoor scenario, with accuracy around 3 meters. This precision is not enough to drive a wheelchair autonomously. Additionally, it is well-known that the GPS was not designed to work inside a building. For this reason, a new indoor positioning IPS for our wheelchair is presented. Our new system was built with some Wi-Fi ESP8266 modules and a Raspberry Pi to drive directional motorized antennas which gather longitudinal and latitudinal coordinates using a triangulation approach described in the next section.

Low cost Yagi antennas have been used in the present study since the use of an array of static antennas is expensive. The angles of at least two Wi-Fi Yagi antennas are used to make a triangulation process. Flores, Marcillo, and Pereira, in 2017, utilized a comparable system to assess the position of a drone. Now, the same positioning system is reused with the IPL/IT autonomous wheelchair. The wheelchair can be manipulated by sending commands to the main server from a mobile app. The server then passes these commands to the hardware actually connected to the Internet via the Wi-Fi network which then generates suitable signals to guide the wheelchair. Figure 6 depicts our Wi-Fi Yagi antenna system printed in a 3D printer.

Three directional antennas with a microcontroller ESP8266 are positioned on two servo motors which have a range of 180 degrees. In our scenario, the wheelchair is located inside a geographical equilateral triangle of 5 meters. The IoT (Internet of Things) technologies with 3 ESP8266 modules (Fig. 7) are placed at the vertices of the triangle. It is possible, in this manner, to discover the location of the wheelchair with a minimum error of few centimeters.

As mentioned earlier, the objective of the current initiative is to improve the present facilities of the IPL/IT wheelchair prototype with the intent of enhancing its user-friendliness, robustness, and accountability to enable both users. This initiative uses IoT technologies to enhance the earlier IPL/IT wheelchair system. The primary elements of the extended system are: a centralized server with a Raspberry PI minicomputer for control and a set of servo motors for each ESP8266 antenna. A Wi-Fi network of ESP8266 modules was used to obtain the wheelchair location. All the modules are distributed in a real indoors scenario and they use Wi-Fi to communicate with the wheelchair server.

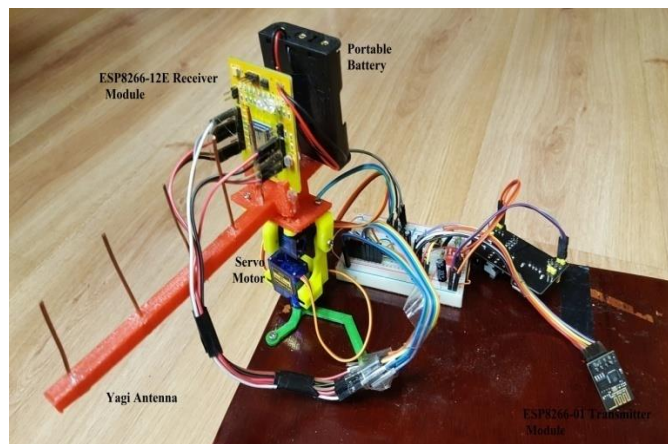


**Figure 6:** Wi-Fi Yagi antenna for an accurate indoor positioning system (prototype)

### III. TRIANGULATION PROCESS

The positional coordinates are achieved using the Angle of Arrival (AoA) method (Fig. 7). This work suggests a novel location method using Wi-Fi ESP8266 modules and Yagi motorized antennas. For the AoA setup, the angles  $\theta_1$  and  $\theta_2$  of the Fig. 8 are measured for all nodes (here, P1 and P2). Then, the line representing the orientation of highest received RF power is accessed by all antennas, their coordinates  $(X_i, Y_i)$ ,  $i=1, 2$  and the angles  $\theta_1$  and  $\theta_2$  (being known). The intersecting point of the lines  $S(X, Y)$  is arrived at as follows [37]:

$$\text{For line } P_1S, \text{ slope} = \tan\theta_1 = \frac{Y-Y_1}{X-X_1},$$

we obtain:

$$Y = X \tan\theta_1 + Y_1 - X_1 \tan\theta_1. \quad (1)$$

Again, for line P<sub>2</sub>S, slope =  $\tan\theta_2 = \frac{Y - Y_2}{X - X_2}$ .

Rearranging, we obtain:

$$Y = X \tan\theta_2 + Y_2 - X_2 \tan\theta_2. \quad (2)$$

Solving for X and Y, we get:

$$X = \frac{X_1 \tan\theta_1 - X_2 \tan\theta_2 + Y_2 - Y_1}{\tan\theta_1 - \tan\theta_2}. \quad (3)$$

Similarly, we obtain:

$$Y = \frac{(X_1 - X_2)\tan\theta_1 \tan\theta_2 - Y_1 \tan\theta_2 + Y_2 \tan\theta_1}{\tan\theta_1 - \tan\theta_2}. \quad (4)$$

Thus, the coordinates of S (of the wheelchair) are:

$$S = \left( \frac{X_1 \tan\theta_1 - X_2 \tan\theta_2 + Y_2 - Y_1}{\tan\theta_1 - \tan\theta_2}, \frac{(X_1 - X_2)\tan\theta_1 \tan\theta_2 - Y_1 \tan\theta_2 + Y_2 \tan\theta_1}{\tan\theta_1 - \tan\theta_2} \right). \quad (5)$$

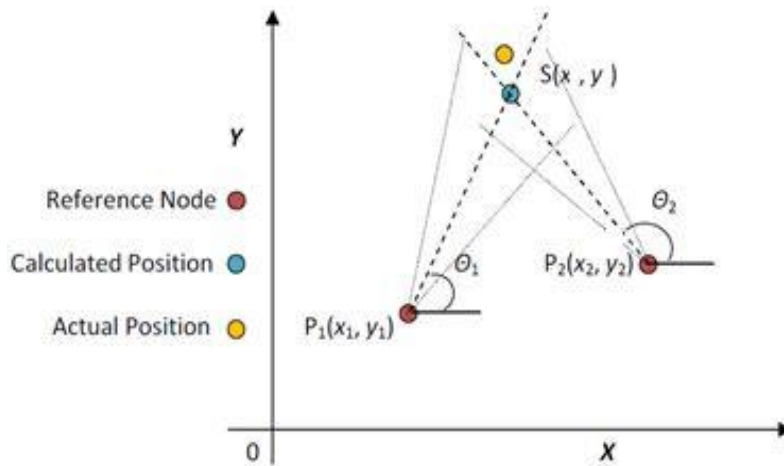
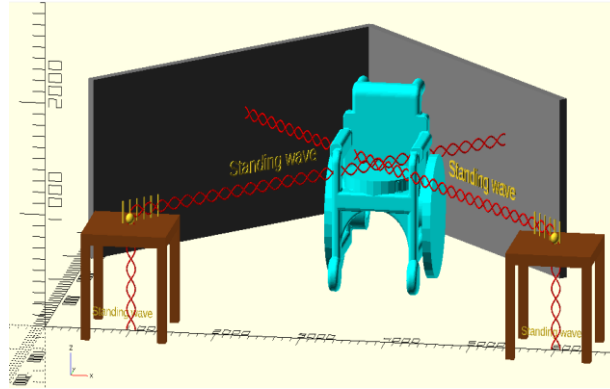


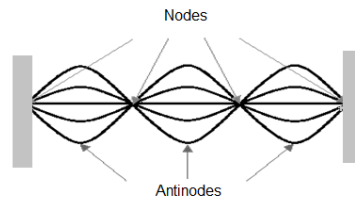
Figure 7: Triangulation method using AoA

In wireless communications, multipath is a phenomenon of propagation in which the same radio signal arrives at the receiving antenna through more than one path. It results in multipath interference (MPI), which may be constructive and destructive interference, and causes the phase of the signal to get shifted. In this work, two Radio Frequency (RF) emitters (ESP8266 with Yagi antennas) are placed on the tables as illustrated in Fig. 8. Standing waves can be created when obstacles are placed in the path of a direct wave. The floor, for instance, can generate a standing wave by reflection of the direct wave. Similarly, a wheelchair or the walls, as obstacles, can generate many standing waves by causing a reflection of a direct wave. To overcome these issues, our positioning system uses a new method for cancelling standing waves [38]. This enhances the positional accuracy of obstacles and minimizes the effects of standing waves. In Fig. 9, the system attempts to accurately locate the wheelchair. The wheelchair has a Wi-Fi module that is used to identify the real location, by mean of the triangulation process described earlier. Each Wi-Fi directional antenna makes a scan of over 180 degrees until it discovers the angle that has the highest power received by the Wi-Fi emitter on the wheelchair.



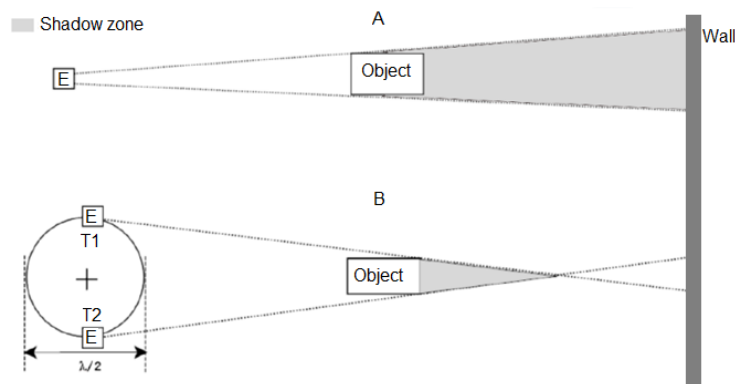
**Figure 8:** Standing waves created by obstacles (scale: mm)

Figure 9 depicts a graph displaying the formation of a specific standing wave. The standing wave effect has a major impact on the accuracy of location estimation in a radio wave based system, due to the constant change in amplitude of the wave that affects signal strength readings, and thus, location accuracy. The standing wave is a wave with a full wavelength  $\lambda$ , where  $\lambda$  is also the wavelength of the RF carrier. To mitigate the effect of the standing waves, we use hardware-based methods to generate two different waves, in our pending patent [30]. The method generates a second wave with a variable delay that reduces the slow fluctuation of the standing wave.



**Figure 9:** Formation of a standing wave

Figure 10 shows a method to reduce the standing waves effect and the RF shadow zone (grey zone) that can be useful on positioning estimation. The standing wave phenomenon has a detrimental influence on the estimation accuracy when radio waves are used since wave amplitude varies constantly, thus affecting signal strength, and finally, the positional accuracy. To overcome the standing-wave effect, a hardware-oriented technique has been carried out to move the RF emitter in order to mitigate the standing wave effect, in our 3 pending patents [38–40]. In resume, it is a simple method that consists to move the initial location of an RF emitter around a circle of half wavelength ( $\lambda/2$ ).



**Figure 10:** Mitigation of a standing wave and reduction of RF shadow zone by moving the initial position of an emitter (E)

A 2D positioning system was set up for optimal transmission and reception of data to study system accuracy and location error. Our IPS uses an automatic rotation of the Yagi antennas that performs a full scan of our indoor scenario, where the wheelchair is located.

As it can be seen in Fig. 9, the two ESP8266RF emitters with Wi-Fi Yagi antennas was located at 5 meters. It is seen from Table 1 that the error, in the 3 different scenarios, increases with growth in antenna distances from the wheelchair. The average error of the three experiments was 30 cm. With the application of the patent pending

technique [30] the error is reduced 46%. Tables 1 and 2 present the outcome of the above experiment conducted in a 5 m x 5m environment in a closed room. The results show that the pending patents technique [38] and [39] significantly improves the accuracy of the wheelchair positioning.

**Table 1:** Indoor location error results

Initial position (X, Y) of the wheelchair [m]	Calculated starting position [m]	Initial error [m]	Final position [m]	Calculated final position [m]	Final error [m]	Average of the new error [m]	% of error location improvement after applying the pending patents [38] and [39]
(2.3, 2.7)	(2.59, 2.207)	0.57	(5.6, 5.85)	(5.15, 5.42)	0.49	0.30	46
(2.6, 2.9)	(2.85, 3.43)	0.58	(2.95, 2.71)	(3.11, 2.39)	0.35		
(2.2, 3)	(1.89, 1.13)	0.33	(1.99, 2.7)	(1.99, 2.76)	0.05		

**Table 2:** Outdoor location error results

Initial position (X, Y) of the wheelchair [m]	Calculated starting position [m]	Initial error [m]	Final position [m]	Calculated final position [m]	Final error [m]	Average of the new error [m]	% of error location improvement after applying the pending patents [38] and [39]
(1.72, 1.11)	(1.67, 1.11)	0.04	-	-	-	0.14	33%
(1.23, 0.87)	(1.16, 0.88)	0.10	(2.80, 2.13)	(2.86, 2.25)	0.07		
(1.39, 1.15)	(1.23, 1.12)	0.20	(2.11, 2.58)	(2.29, 1.60)	0.12		
(2.35, 3.53)	(2.15, 3.20)	0.39	(5.10, 4.80)	(5.03, 5.04)	0.25		

#### IV. SOUND CONVERSION OF 3D OBJECTS FOR THE IPL/IT EPW

A new surround 3D headphones device is presented in this section. It uses 3D sounds with a 3D headphone to reproduce consecutive 2D images. By hearing 3D sounds, the user will know not only the shape of an object, but also the depth of it. Through the use of a 3D scanner, it is possible to create 3D objects of the environment in front of the IPL/IT wheelchair. With our new method, the surface of the object is virtually covered by multiple virtual sound sources. For each virtual sound source, located on the surface of the object, a distance is calculated between the user and this source. These distances are calculated to simulate the locations of the various sound sources from the three-dimensional space that reach three pairs of speakers assembled in a new 3D headphone. The sound signals propagate ideally in a homogeneous medium transmission without obstacles, distortions and reflections. The 3D scanned object is decomposed into multiple parallel front layers that are accessed/used sequentially, with a periodic scan performed from the nearest to the farthest layer. Different audible frequencies are used to determine each of the frontal layers. The curves of each layers (cutting the object) are represented by a limited number of points that are used to simulate the origin of the sound sources in a three-dimensional space.

The IPL/IT EPW uses a ©Microsoft Kinect scanner to capture 3D objects and convert them into 3D sounds. This converter is designed based on our pending patent [41]. All objects can be scanned and modeled by a decomposition of layers in a 3D Cartesian system (Fig. 11). The next step is to use images of the shape of the object in each layers (several parallel plans along the z-axis. Each layer is identified by an assigned specific set of audio frequencies. Every parallel layer is mapped on a 2D plan which contains the contour of the object. All such curves are identified by a collection of points that simulate an acoustic signal source in the 3D space. The virtual point locations of virtual sound sources are represented by 2D polar coordinates (radius =  $R$  and angle =  $B$ ) centered on a horizontal line passing through the center of the three-dimensional object space and parallel to the X-Y plane. The points of virtual location of each sound source have equal audible frequencies whenever the  $R$  rays are equal, despite the angles  $B$  being different in the range 0–360°. The virtual points with high  $R$  are represented by low audible frequency range and points with low  $R$  are represented by higher audible frequencies. The user can estimate the object shape based on the hearing of an audible frequency proportional to the radius  $R$  on each plane.



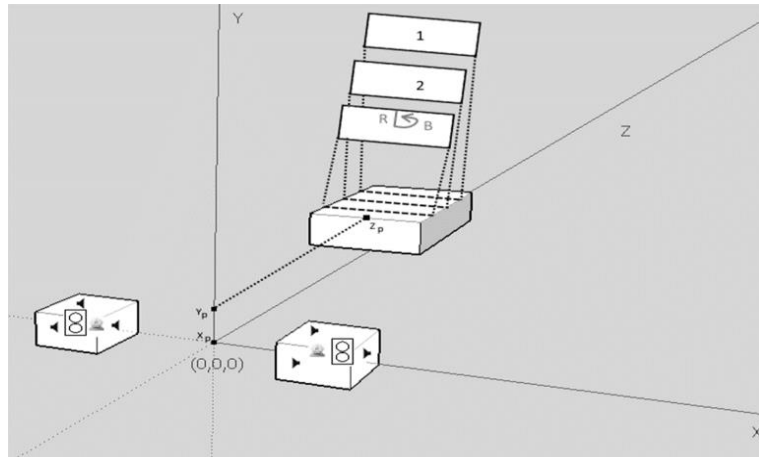


**Figure 11.** 3D object decomposition, by layer, on a Cartesian system

To generate a particular sound for a particular speaker, the Euclidean separation between each point and each speaker  $p(x_p, y_p, z_p)$  is calculated as follows:

$$D = \sqrt{(x_p - x_{speaker})^2 + (y_p - y_{speaker})^2 + (z_p - z_{speaker})^2} \quad (6)$$

This distance  $D$  is used to generate the cosine sound wave for the corresponding speaker using the formula for displacement  $y(t)$  as:

$$y(t) = 256 * e^{-D} * \cos\left(\left(\frac{v}{D} * \frac{2\pi}{10^{-6} * D}\right) + (2\pi / (10^{-6} * D)) * \frac{t}{f}\right) \quad (7)$$

The experiments were carried out using the frequency  $f = 44.1$  kHz. The velocity of sound in air was taken to be  $v = 340$  m/s.

The software responsible for the generation of the sound starts by capturing the scenario or an object using a ©Microsoft Kinect 3D scanner. After the 3D object is generated, it is separated into various layers and the nearest layer is selected first. The outline of the object for that layer is represented in a 2D array, with the position of the array matching the outline of the object having a value (depth value) defined for that layer and the other positions having zero as value. The angle and radius of each sound source are calculated for each selected layer. After all, the angles and radius are calculated, the sound for each one of the 6 speakers (RB, RU, RD, LB, LU, LD) is generated (Fig. 12). When generation of all 6 sounds is finished, the left group of speakers plays the sounds generated for LB, LU and LD, while the right side plays the sounds for RB, RU and RD and then the software moves to the next layer. This process is repeated until the software reaches the farthest layer from the user. If, after all layers have been processed, our software detects any movement, this whole process will be repeated. Figure 12 can be used to better understand the previous method that it is described in the algorithm of Fig. 13.

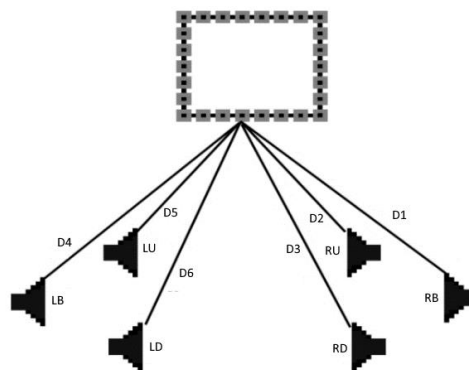


**Figure 12:** Distance between speakers and points

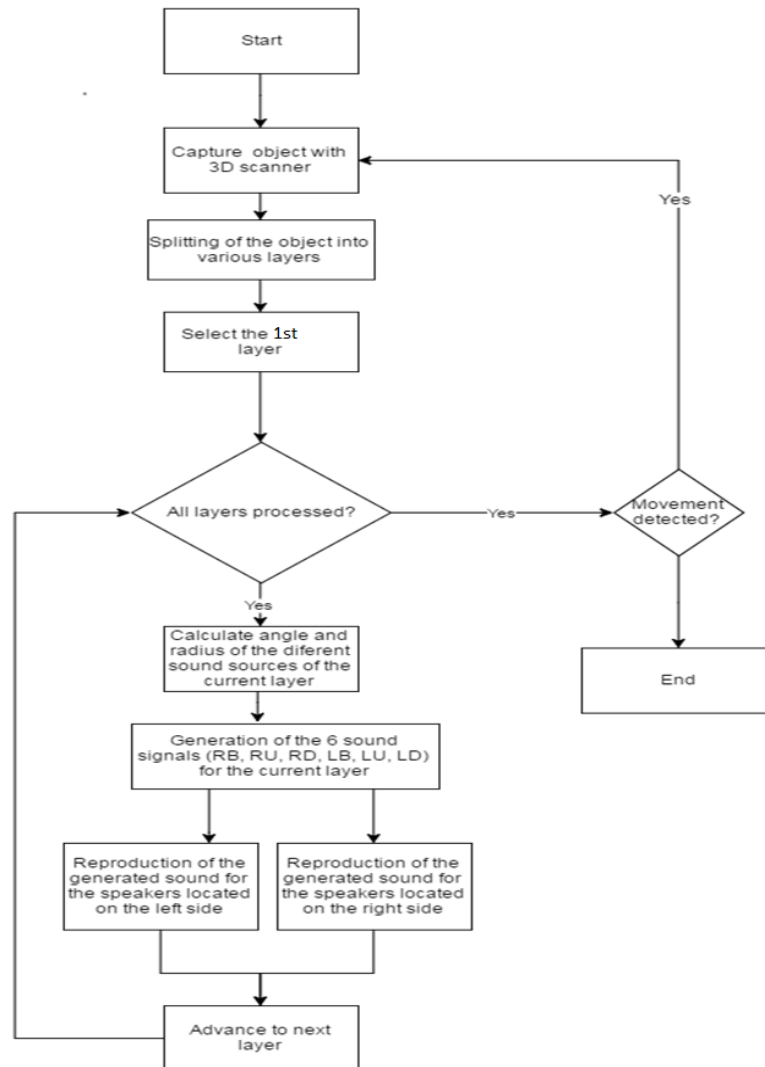


**Figure 13:** Algorithm diagram

Figures 14–16 illustrate scans of a person making a hand gesture movement, a semi-closed door, and a closed door, respectively. The 3D objects are shown in the left, the scanned images converted into frequency sounds in the right (a different color for each frequency) and the generated sound amplitude below (delivered to 6 different pair of speakers). The colored points of the scanned images represent sounds of different frequencies, for all layers. Comparing these three figures, we observe that the more the variation in depth, the longer the duration of sound. After some training, using the 3D headphone of Figure 4, a blind person was able to easily recognize the three different objects. However, it may be possible to recognize other objects if intensive training is provided. In this paper we proposed a solution to convert 3D objects into sound to give visually impaired people an idea of what an object looks like and how distant it is. Compared to other solutions that use 2D images, the use of a 3D object gives us a better understanding of that object. Instead of using the intensity of the pixels of an image to generate a sound to describe the image, our method (pending patent [41]) uses separate layers of the object to give visually impaired people a better understanding of the object’s shape and depth.

To test this solution, a small group of 5 people was selected. The test consisted in playing the sounds of the closed and the semi-closed doors five times each with the person listening to the sound knowing to which object that sound corresponded to. After listening to all ten sounds, each person was given ten new sounds, five of a different closed door and five of a different semi-closed door, in a random order and had to guess which sound corresponded to which object. The test group managed to guess the right object 84% of the time.

With the tests performed, it was possible to identify not only the shape of the object, but also to identify its location in a 3D space. In the future, we intend to move the current computer application to a more portable solution. Along with this portable device, we also intend to take more tests with other real obstacles facing the autonomous IPL/IT wheelchair.

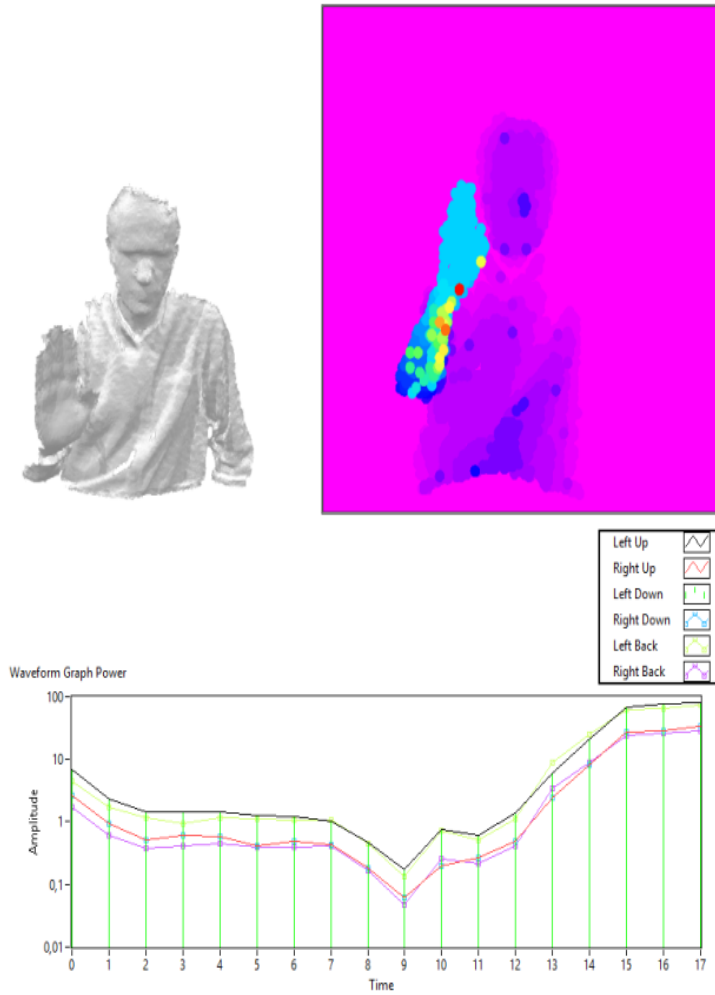


Figure 14: Audible scan of a person

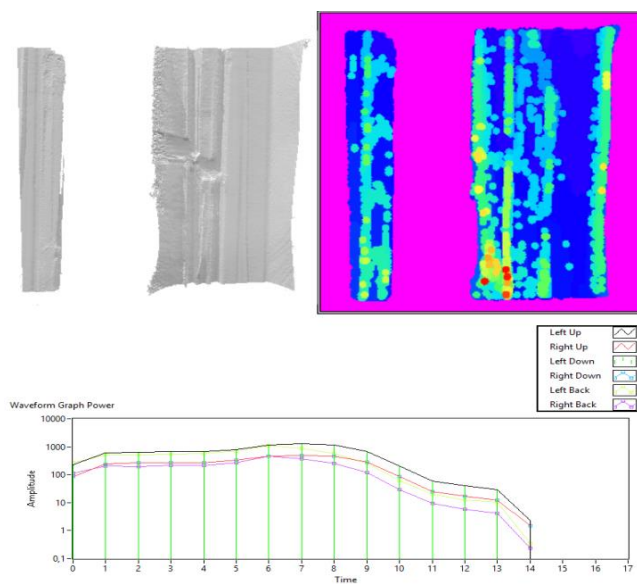


Figure 15: Audible scan of a semi-closed door

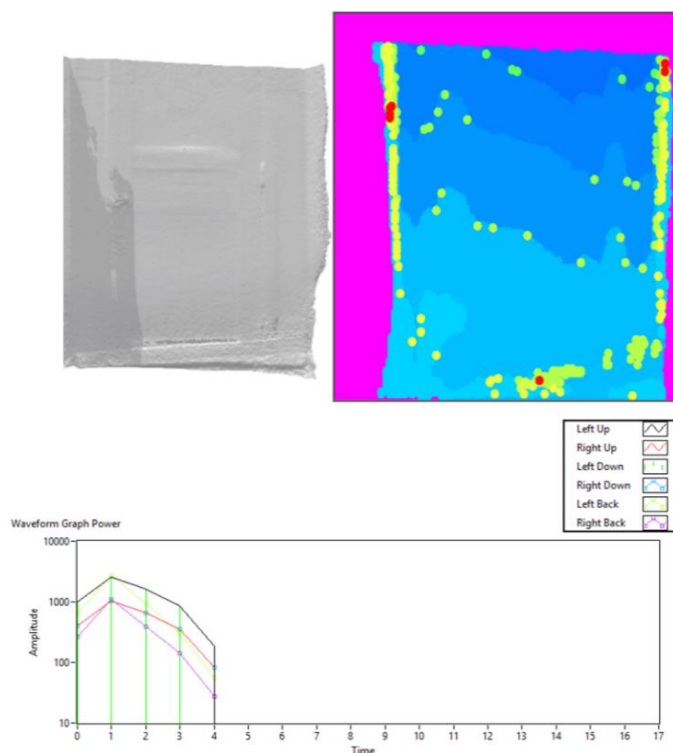


Figure 16: Audible scan of a closed door

## V. CONCLUSIONS

In this study, a smart autonomous wheelchair (IPL/IP EPW) having voice and eye-movement control has been described. The system uses a Wi-Fi network of ESP8266 modules to implement an accurate positioning system. This new system, based on some pending patents, has been tested successfully. The proposed system presents the location of a wheelchair with a positioning accuracy around 30 cm, when the experiment is performed within an indoor scenario. In addition, the IPL/IT EPW has been fitted with a novel 3D scanner that generates 3D sound appropriate to the obstacle sensed. This feature combined with the proposed positioning system will be beneficial to the visually challenged.

## ACKNOWLEDGEMENT

The authors would like to thank the following students for their contributions, building the previous IPL/IT EPW prototype: Catarina Curioso, Duarte Ferreira, Flávia Simão, Inês Grenha, Mauro Pinheiro, Nuno Santos, Sílvia Fernandes, Tiago Neves, Guilherme Nunes, Fábio Matos, Nuno Domingues, Maurício Quaresma, Rui Paiva, Micael Florêncio, Ricardo Ferreira, João Santos, Christophe Silva, Virgílio Reis, Rui Vieira, João Silva, Elza Sousa, and Pedro Silva. Additionally, we would like to thank to the Professors Ricardo Martinho, Pedro Martinho, and Patrício Domingues. Finally, we thank the Polytechnic Institute of Leiria, School of Technology and Management of Leiria, and the “Instituto de Telecomunicações” of Portugal.

## REFERENCES

- [1]. World Health Organization [WHO]. (2017) *Guidelines on the provision of manual wheelchairs in less-resourced settings*. Available from: <http://www.who.int/disabilities/publications/technology/wheelchairguidelines/en/> [Accessed 14th November 2017].
- [2]. N. Thapar, G. Warner, M.L. Drainoni, S.R. Williams, H. Ditchfield, J. Wierbicky, and S. Nesathurai, “A pilot study of functional access to public buildings and facilities for persons with impairments,” *Disabil. Rehabil.*, 26(5), 2004, 280-289.
- [3]. R. C. Simpson, “How many people would benefit from a smart wheelchair?,” *J. Rehabil. Res. Dev.*, 45(1), 2008, 53–72.
- [4]. M.H. Alsibai and S.A. Manap, “A Study on Smart Wheelchair Systems,” *Int. J. Eng. Technol. Sci.*, December 2015.
- [5]. R. C. Simpson, “Smart wheelchairs: A literature review,” *J. Rehabil. Res. Dev.*, 42(4), 2005, 423.
- [6]. U. Borgolte, H. Hoyer, C. Bühler, H. Heck, and R. Hoelper, (1998) “Architectural concepts of a semi-autonomous wheelchair,” *J. Intell. Robot. Sys.*, 22(3), 1998, 233–253.

- [7]. N. Katevas, N. Sgouros, S. Tzafestas, G. Papakonstantinou, P. Beattie, J. Bishop, P. Tsanakas, and D. Koutsouris, "The autonomous mobile robot SENARIO: a sensor aided intelligent navigation system for powered wheelchairs," *IEEE Robot. Autom. Mag.*, 4(4), 1997, 60–70.
- [8]. R. C. Simpson, S. P. Levine, D. A. Bell, L. A. Jaros, Y. Koren, and J. Borenstein, "NavChair: An assistive wheelchair navigation system with automatic adaptation," *Assistive Technology and Artificial Intelligence Lecture Notes in Computer Science*, 235–255.
- [9]. E. Prassler, J. Scholz, and P. Fiorini, "A robotics wheelchair for crowded public environment," *IEEE Robot. Autom. Mag.*, 8(1), 2001, 38–45.
- [10]. M. Mazo, "An integral system for assisted mobility [automated wheelchair]," *IEEE Robot. Autom. Mag.*, 8(1), 2001, 46–56.
- [11]. D. P. Miller and M. G. Slack, "Design and testing of a low-cost robotic wheelchair prototype," *Auton. Robots*, 2(1), 1995, 77–88.
- [12]. R.C. Simpson, E.F. LoPresti, S. Hayashi, S. Guo, D. Ding, and R.A. Cooper, "Smart Power Assistance Module for manual wheelchairs. Technology and Disability: Research, Design, Practice and Policy," in *26th International Annual Conference on Assistive Technology for People with Disabilities (RESNA)*, June 2003.
- [13]. R. Simpson, E. Lopresti, S. Hayashi, I. Nourbakhsh, and D. Miller, "The Smart Wheelchair Component System," *J. Rehabil. Res. Dev.*, 41(3), 2004, 429.
- [14]. R. Simpson, D. Poirot, and F. Baxter, "The Hephaestus Smart Wheelchair system," *IEEE Trans. Neural Syst. Rehabil. Eng.*, 10(2), 2002, 118–122.
- [15]. Lankenau and T. Röfer, "Smart Wheelchairs - State of the Art in an Emerging Market," *KI*, 14(4), 2000, 37-39.
- [16]. G. Bourhis and M. Sahnoun, "Assisted control mode for a smart wheelchair." in *Rehabil. Robot., 2007. ICORR 2007. IEEE 10th Int. Conf.*, June 2007, 158–163.
- [17]. D. M. Brienza and J. Angelo, "A force feedback joystick and control algorithm for wheelchair obstacle avoidance," *Disabil. Rehab.*, 18(3), 1996, 123–129.
- [18]. L. Fehr, W.E. Langbein, and S.B. Skaar, "Adequacy of power wheelchair control interfaces for persons with severe disabilities: A clinical survey," *J. Rehabil. Res. Dev.*, 37(3), 2000, 353.
- [19]. T. Felzer and R. Nordmann, "Alternative wheelchair control," in *Proc. 1st Int. IEEE-BAIS Symp. Res. Assistive Technol.*, 7, 2007, 67–74.
- [20]. H. Li, M. Kutbi, X. Li, C. Cai, P. Mordohai, and G. Hua, "An egocentric computer vision based co-robot wheelchair," in *IEEE/RSJ Int. Conf. Intell. Robots Syst. (IROS)*, 2016, 1829–1836.
- [21]. P.C. Hsieh, "Autonomous robotic wheelchair with collision-avoidance navigation," M.S. thesis, Texas A&M Univ., 2008.
- [22]. E. Prassler, J. Scholz, M. Strobel, and P. Fiorini, "An intelligent (semi-) autonomous passenger transportation system," in *Proc. 199 IEEE/IEEJ/JSAI Int. Conf. Intell. Transport. Syst.*, Oct 1999, 374–379.
- [23]. R. Tang, "A Semi-autonomous Wheelchair Navigation System," M.S. Thesis, Univ. of Canterbury, 2012.
- [24]. S. Hemachandra, T. Kollar, N. Roy, and S. Teller, "Following and interpreting narrated guided tours," in *2011 IEEE Int. Conf. Robot. Autom.*, 2011.
- [25]. H. Wakaumi, K. Nakamura, and T. Matsumura, "Development of an automated wheelchair guided by a magnetic ferrite marker lane," *J. Rehabil. Res. Dev.*, 29(1), 1992, 27.
- [26]. Borenstein, J., Everett, H.R., Feng, L., Lee, S.W., Byrne, R.H.: *Where am I? Sensors and Methods for Mobile Robot Positioning*. University of Michigan, 1996.
- [27]. Yazıcı, A., Parlaktuna, O.: Mobile robot localization using laser range finder and artificial landmark. In: *Proceedings of IKECCO'2005*, 129–133.
- [28]. Rencken, W.D.: Concurrent localization and map building for mobile robots using ultrasonic sensors. In: *Proceedings of the 1993 IEEE/RSJ International Conference on Intelligent Robotics and Systems*, Yokohama 1993, 2192–2197.
- [29]. Barnes, J., Cranenbroeck, J.V., Rizos, C., Pahwa, A., Politi, N.: Long term performance analysis of a new groundtransceiver positioning network (LocataNet) for structural deformation. In: *FIG Working Week 2007*. Hong Kong SAR, 2007.
- [30]. Q-Track: [www.q-track.com](http://www.q-track.com). Accessed 18 Dec 2012.
- [31]. S.A. Dallas Jr and A.J. Erickson, "U.S. Patent No. 4378569," Washington, DC: U.S. Patent and Trademark Office, 1983.
- [32]. W.E. Langbein and L. Fehr, "Research device to preproduction prototype: a chronology," *J Rehabil Res Dev*, 30(4), 1993, 436.
- [33]. The Voice, "Augmented reality for the totally blind," September 2017, unpublished.

- [34]. J. Pereira, R. Monteiro, H. A. Silva, J. Lopes, Correlation of STFT Spectrograms Applied to Voice Deal Function in Mobile Phones, *WSEAS International Conf. on Appl Mathematics and Computer Science*, Athens, Greece, 1, December, 2001, 65 – 68.
- [35]. J.P. Espada, O.S. Martínez, J.M.C. Lovelle, B.C.P. G-Bustelo, M.A. Álvarez, and A.G. García, “Modeling architecture for collaborative virtual objects based on services,” *J. Netw. Comput. Appl.*, 34(5), 2011, 1634–1647.
- [36]. L. A. Amaral, F. P. Hessel, E. A. Bezerra, J. C. Corrêa, O. B. Longhi, and T. F. Dias, “eCloudRFID – A mobile software framework architecture for pervasive RFID-based applications,” *J. Netw. Comput. Appl.*, 34(3), 2011, 972–979.
- [37]. Z. Shan and T.-S. P. Yum, “Precise Localization with Smart Antennas in Ad-Hoc Networks,” *IEEE GLOBECOM 2007-2007 IEEE Global Telecommunications Conference*, 2007.
- [38]. J. Pereira, J.B. Bagaric, and S. P. M. Mendes, “Standing Wave Cancellation – Wireless Transmitter, Receiver, System and Respective Method,” *Patent 109137*, February, 2016, (Pending).
- [39]. J. Pereira, M.G. Gasparovic, Pooja M., and G. Manjunath, “Standing Wave Cancellation and Shadow Zone Reducing Wireless Transmitter, System and Respective Method and Uses,” *Patent 109332*, April, 2016, (Pending).
- [40]. J. Pereira, M.G. Gasparovic, and M. P. M. Ferreira, “Indoor Positioning System and Method,” *Patent 109950*, March, 2017, (Pending).
- [41]. J. Pereira and N. M. L. Almeida, “Método e Aparelho de Criação de um Cenário Tridimensional,” *Patent 109485*, July, 2016 (Pending)

IOSR Journal of Engineering (IOSRJEN) is UGC approved Journal with Sl. No. 3240, Journal no. 48995.

João S. Pereira. "An Autonomous Wheelchair with Indoor Positioning System and Smart 3D Headphone for the Visually Impaired." *IOSR Journal of Engineering (IOSRJEN)*, vol. 09, no. 2, 2019, pp. 27-40.